

## MICROELECTRONIC DEVICES AND SYSTEMS

# $f_T \times BV_{cbo}$ Product Modeling for SiGe:C HBTs<sup>1</sup>

K. O. Petrosjanc and R. A. Torgovnikov

Moscow Institute of Electronics and Mathematics (Technical University), MIEM,  
Bolshoy Trehsvyatitskiy per. 3, Moscow, 109028 Russia

e-mail: torrosj@rambler.ru

Received January 12, 2009

**Abstract**—The specific aspects of SiGe:C HBT process and device simulation using TCAD are discussed. Cut-off frequency  $f_T$  and collector junction breakdown voltage  $BV_{cbo}$  dependences on carbon concentration in SiGe base area are investigated. The boron and carbon profiles in SiGe base are obtained to provide a trade-off between gain, cut-off frequency and break-down voltage. High values of  $f_T \times BV_{cbo}$  product were achieved.

PACS numbers: 85.30.-z, 85.30.Pq, 85.30.De

DOI: 10.1134/S106378260913020X

### INTRODUCTION

Silicon-Germanium (SiGe) BiCMOS technology is used for more than ten years to produce very high-frequency ICs for variety of consumer electronics—wireless local area networks, automotive radars, cellular phones, optical communications etc. [1–6]. SiGe offers the opportunity to integrate a high performance HBT with CMOS analog and digital functions on a single chip. The main stream of improving the SiGe BiCMOS technology is maximizing HBT performance. There are several ways to improve SiGe HBT parameters:

—formation of self-aligned structures to decrease parasitic capacitances;

—use of selective epitaxy to achieve full self-aligned device;

—optimization of germanium profile in base and collector regions;

—incorporation of the carbon in base and collector layers to prevent a boron out-diffusion into the base region and parasitic potential barrier near collector-base junction;

—reduction of base and collector resistances;

—device layout optimization.

Simultaneous use of these methods allows to create modern high speed HBTs. World-famous companies IBM [1–3], STM [4], Philips [5], Hitachi [6], Sony [7] etc. produce SiGe:C BiCMOS LSIs. Nowadays the peak values of cut-off frequency  $f_T$  are about 200–230 GHz [2, 4] and the values of 300–350 GHz are expected in nearest future [3].

One of the most effective technological options is carbon incorporation in SiGe HBT's base region. A major concern in SiGe HBT fabrication is the broadening of the SiGe base boron profile due to out-diffusion of boron into neighboring Si emitter and collector regions. This outdiffusion significantly degrades device performance. An effective technique to suppress this is to incorporate localized substitutional carbon in the base of SiGe HBT.

Incorporation of low concentrations of carbon into the base region of a  $Si_{1-x}Ge_x$  HBT can dramatically suppress boron outdiffusion, thus paving the way for further improvements in SiGe HBT performance. In essence, it leads to reduction of the base region width (see Fig. 1), that significantly increases the value of

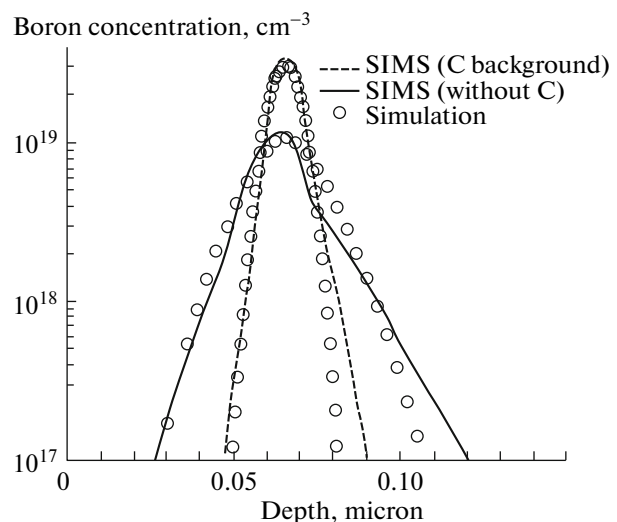


**Fig. 1.** SIMS profiles of boron in the base of SiGe HBT with a carbon background (dashed line) and without carbon (solid line) [8].

<sup>1</sup> The article was translated by the authors.

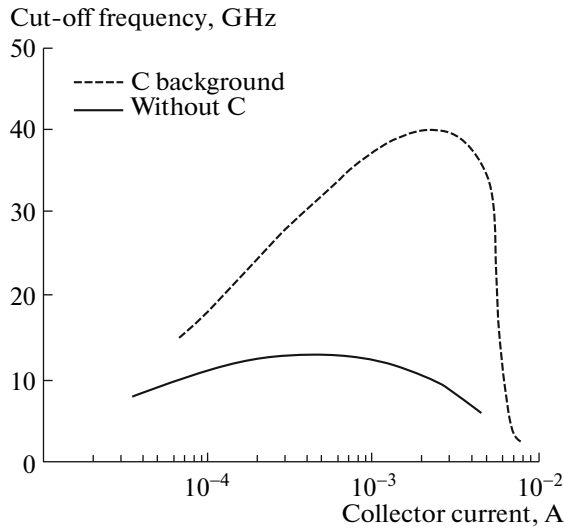


Fig. 2. Cut-off frequency  $f_T$  vs. collector current for HBT with a carbon background (dashed line) and without carbon (solid line) [8].

cut-off frequency peak  $f_T$  (see Fig. 2) [8]. The diffusion coefficient of boron in SiGe is reduced by more than one order of magnitude. The reduced boron diffusion also enables a much higher base doping to be used with intrinsic base resistance value. Highly-doped SiGe:C HBTs in comparison with C-free HBTs demonstrate increased cut-off ( $f_T$ ) and maximum oscillation ( $f_{max}$ ) frequencies by 50–70%, and reduced RF noises and ring oscillators delays. Moreover emitter dimensions can be shrunk to reduce power consumption, without loss in RF performance. Incorporation of carbon into the SiGe base layer also reduces the strain, thus improving the thermal stability of SiGe layer. This means that the HBTs with carbon doping is less affected by thermal cycling from CMOS platform technology. SiGe:C HBTs exhibit leakage currents, which are sufficiently low for reliable VLSI applications.

Many authors [8–12] have used TCAD systems to study the parameters of modern SiGe HBTs with carbon doping base. Most of the existing studies for modeling SiGe:C HBTs are exclusively focused on high frequency and lower power performance.

In this study, we use the Synopsys Sentaurus TCAD system for analysis of SiGe:C structures having potential to compete in analogue, mixed signal, RF power ICs and Systems on a Chip (SoC) where a balance between gain, cut-off frequency and breakdown voltage is necessary. The boron and carbon profiles in SiGe base were obtained to provide a trade-off between gain, cut-off frequency and break-down voltage. Large values of  $f_T \times BV_{cbo}$  product were achieved.

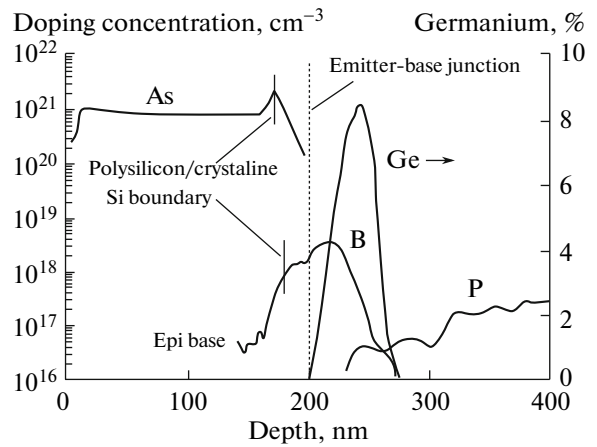


Fig. 3. SiGe HBT profile [1].

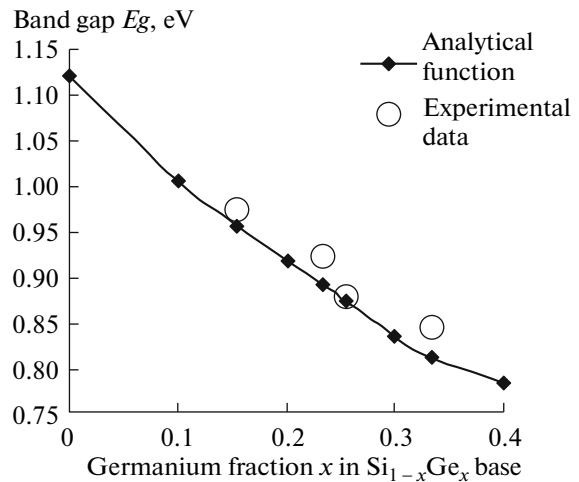


Fig. 4. Band gap  $E_g$  vs. germanium fraction  $x$  for  $Si_{1-x}Ge_x$  base. Comparison of empirical function and experimental data [15].

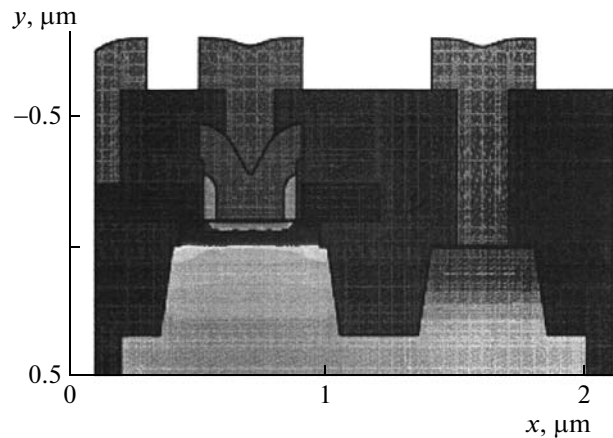


Fig. 5. Simulated SiGe HBT structure.

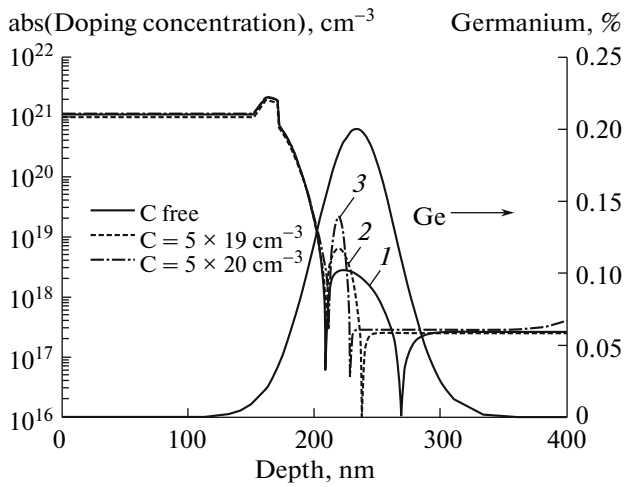


Fig. 6. Simulated doping profiles of SiGe:C HBT for different carbon concentrations in base.

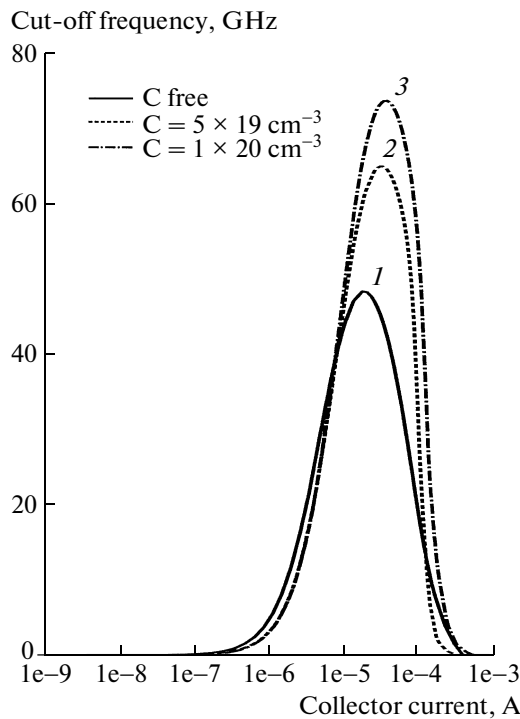


Fig. 7. Simulated cut-off frequencies  $f_T$  vs. collector current.

DEVICE SIMULATION

The standard structure of SiGe:C HBT (Fig. 3) [1] was simulated for different carbon concentrations in the range of  $10^{19} \text{ cm}^{-3}$ – $10^{20} \text{ cm}^{-3}$ .

It was shown [13, 14] that the physical parameters in the  $\text{Si}_{1-x-y}\text{Ge}_x\text{C}_y$  base: diffusivity, band gap energy, recombination rate, carrier lifetime differ from the same parameters in Ge and C-free base of HBT.

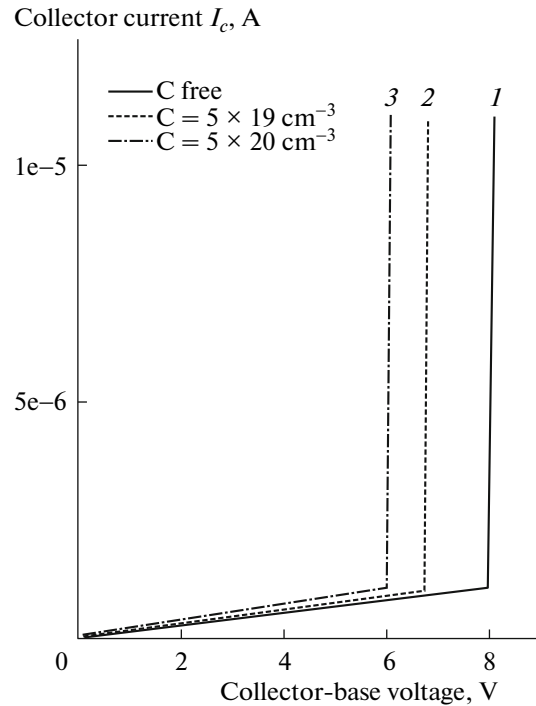


Fig. 8. Simulated reverse-biased characteristics at collector-base junction.

In device simulation we have used suitable physical models for mobility, band gap narrowing, avalanche breakdown, Shockley-Read-Hall and Auger recombination. To describe the relation of  $\text{Si}_{1-x}\text{Ge}_x$  band gap ( $\Delta E_g$ ) with Ge content  $x$  the dependence shown in Fig. 4 was chosen [15]. The difference between simulated and experimental data is less than 5%.

The values of boron diffusivity in SiGe base were determined from experimental data and corrected for every level of carbon doping [8, 9, 13, 16].

In papers [9, 10] boron and carbon diffusion in SiGe:C layers under different actual process conditions, typical for BiCMOS processes, was studied. The authors used two approaches to take into account the influence of carbon on boron diffusion:

(1) experimental carbon profile was used as input data in technological simulation and boron diffusivity was corrected according to carbon concentration in base region [9];

(2) the additional differential equations describing the effect of carbon on boron diffusion were incorporated in TCAD general diffusion model [10].

We have used the Synopsys Sentaurus process simulator which doesn't has diffusion models describing coupled boron diffusion in the presence of germanium and carbon. So in this work the first approach was used for SiGe:C HBT process modeling.

The results of simulation are the following:

(1) SiGe HBT structure (see Fig. 5);

Table

Carbon concentration $C$ , $\text{cm}^{-3}$	0	$5 \times 10^{19}$	$10^{20}$
Peak of boron concentration in base region $N_{\text{BMAX}}$ , $\text{cm}^{-3}$	$3 \times 10^{18}$	$7 \times 10^{18}$	$3 \times 10^{19}$
Base width $W_b$ , nm	60	30	17
DC current gain	90	100	150
Peak of cut-off Frequency $f_T$ , GHz	47	63	72
Collector-base breakdown voltage $BV_{\text{CBO}}$ , V	7.9	6.7	6.0
$f_T \times BV_{\text{CBO}}$ product	355	420	432

(2) doping profiles of SiGe:C HBT for different carbon concentrations (see Fig. 6);

(3) corresponding values of peak cut-off frequency  $f_T$  (Fig. 7) and collector junction breakdown voltage  $BV_{\text{cbo}}$  (Fig. 8).

It should be pointed out that in SiGe:C HBT with carbon doping level increasing simultaneously with the rise of cut-off frequency peak  $f_T$  significant degradation in breakdown voltages  $BV_{\text{cbo}}$  is observed. Therefore investigation of dependence of  $BV_{\text{cbo}}$  on carbon doping level of  $\text{Si}_{1-x-y}\text{Ge}_x\text{C}_y$  base is one of the goals of this work.

Figure 6 illustrates the degradation of the base width of HBT structures width decreased from 60 nm (for conventional SiGe HBT,  $C = 0$ ) to 18 nm (for SiGe:C HBT). For carbon concentration  $C = 5 \times 10^{19} \text{ cm}^{-3}$  the peak concentration of boron in base region is  $7 \times 10^{18} \text{ cm}^{-3}$  (profile 2), and for carbon  $C = 10^{20} \text{ cm}^{-3}$  this peak value is about  $3 \times 10^{19} \text{ cm}^{-3}$  (profile 3).

Figure 7 presents the dependences of cut-off frequency peak  $f_T$  on collector current density for various carbon profiles. The maximum value of  $f_T$  rises from 45 GHz for  $C = 0$  (profile 1) to 63 GHz for  $C = 5 \times 10^{19} \text{ cm}^{-3}$  (profile 2), and to 72 GHz for  $C = 10^{20} \text{ cm}^{-3}$  (profile 3).

Figure 8 presents current–voltage curves of reverse-biased collector  $p$ – $n$ -junction. Breakdown voltages are shown: 7.9 V for conventional SiGe HBT without carbon introduction,  $C = 0$  (profile 1); 6.7 V for  $C = 5 \times 10^{19} \text{ cm}^{-3}$  (profile 2) and 6.0 V for  $C = 10^{20} \text{ cm}^{-3}$  (profile 3).

The values of  $f_T \times BV_{\text{cbo}}$  product are given in the table. It is seen that balanced combinations of main parameters for SiGe:C HBT are achieved for both carbon concentrations  $5 \times 10^{19} \text{ cm}^{-3}$  and  $10^{20} \text{ cm}^{-3}$ .

## CONCLUSIONS

The features of SiGe:C HBT structures were investigated. The effects of carbon doping in SiGe base were introduced in the technological model to take into account the features of SiGe:C HBT. These effects were built-in Sentaurus Synopsys TCAD in the form of empirical dependences of diffusivity and band

gap in base and  $p$ – $n$  junctions regions on carbon concentration.

It was shown that introduction of low amount of carbon dopant into  $\text{Si}_{1-x-y}\text{Ge}_x\text{C}_y$  base region noticeably increases the value of cut-off frequency  $f_T$  from 45 to 72 GHz, but at the same time decreases breakdown voltage of collector junction  $BV_{\text{cbo}}$  from 7.9 to 6.0 V. For practical reasons the compromise combinations of base width  $W_b$ , carbon concentration  $C$ , and peak boron concentration  $N_{\text{BMAX}}$  was chosen to provide high values of cut-off frequency  $f_T$  and reasonable values of breakdown voltage  $BV_{\text{cbo}}$ . High values of  $f_T \times BV_{\text{cbo}}$  product, important for analog and RF power applications, were achieved. The results are in good agreement with experimental data published in [1, 4, 17].

## REFERENCES

1. B. S. Meyerson, "Silicon:Germanium-Based Mixed-Signal Technology for Optimization of Wired and Wireless Telecommunications," IBM Journal of Research and Development **44** (3), 391–407 (2000).
2. B. A. Orner, Q. Z. Lu, B. Rainey, et al., "A 0.13  $\mu\text{m}$  BiCMOS Technology Featuring a 200/208 GHz ( $f_T/f_{\text{MAX}}$ ) SiGe HBT," in *Proceedings of the IEEE Bipolar/BiCMOS Circuits and Technology Meeting, 2003*, pp. 203–206.
3. G. Freeman, J.-S. Rieh, B. Jagannathan, et al., "SiGe HBT Performance and Reliability Trends Through  $f_T$  of 350 GHz," in *Proceedings of IEEE 41st Annual International Reliability Physics Symposium, Dallas, Texas, 2003*, pp. 332–338.
4. P. Chevalier, C. Fellous, and L. Rubaldo, "230 GHz Self-Aligned SiGeC HBT for 90 nm BiCMOS Technology," in *Proceedings of the Bipolar/BiCMOS Circuits and Technology, 2004*, pp. 225–228.
5. P. H. C. Magnee, G. A. M. Hurkx, and P. Agarwal, "SiGe:C HBT Technology for Advanced BiCMOS Processes," in *Proceedings of 12th GaAs Symposium, Amsterdam, 2004*, pp. 243–246.
6. K. Washio, "SiGe HBT and BiCMOS Technologies for Optical Transmission and Wireless Communication Systems," IEEE Trans. Electron Devices **50**, 656–668 (2003).
7. H. Yamagata, S. Yanagawa, T. Komoto, et al., "101 GHz  $f_{T\text{max}}$  SiGe:C HBT Integrated into 0.25  $\mu\text{m}$  CMOS with Conventional LOCOS Isolation," in *Proceedings*

- of *Solid-State Device Research Conference, 2004*, pp. 201–204.
8. H. Ruecker and B. Heinemann, “Modeling the Effect of Carbon Dopant on Boron Diffusion,” in *Proceedings of International Conference Simulation of Semiconductor Processes and Devices, SISPAD, 1997*, pp. 281–284.
  9. S. Decoutere and A. Sibaja-Hernandez, “SiGe:C HBTs: The TCAD Challenge Reduced to Practice,” *Materials Science in Semiconductor Processing* (8), 283–288 (2005).
  10. S. Rizk and Y. M. Haddara, “Modelling the Suppression of Boron Diffusion in Si/SiGe due to Carbon Incorporation,” *Journal of Vacuum Science Technology* **B 24** (3), 1365–1370 (2006).
  11. A. Sadovnikov, C. Printy, T. Budri, et al., “Effects of Boron and Germanium Base Profiles on SiGe and SiGe:C BJT Characteristics,” in *Proceedings of ESSDERC, 2002*, pp. 611–614.
  12. A. Sibaja-Hernandez, Ming Wei Xu, S. Decoutere, H. Maes, “TSUPREM-4 Based Modeling of Boron and Carbon Diffusion in SiGe:C Base Layers under Rapid Thermal Annealing Conditions,” *Materials Science in Semiconductor Processing* (8), 115–120 (2005).
  13. L. Yang, J. R. Walting, R. C. W. Wilkins, et al., “Si/SiGe Heterostructure Parameters for Device Simulations,” *Semiconductor Sci. Technol.* **19**, 1174–1182 (2004).
  14. P. Dollfus, S. Galdin, P. Hesto, and H. J. Osten, “Band Offsets and Electron Transport Calculation for Strained  $\text{Si}_{1-x-y}\text{Ge}_x\text{C}_y/\text{Si}$  Heterostructures,” *J. Materials Sci.* **12**, 245–248 (2001).
  15. R. Braunstein, A. R. Moore, and F. Herman, “Intrinsic Optical Absorption in Germanium-Silicon Alloys,” *Physical Review* **109**, 695–710 (1958).
  16. N. Zangenberg, J. Fage-Pedersen, J. Lundsgaard, “Boron and Phosphorus Diffusion in Strained and Relaxed Si and SiGe,” *Journal of Applied Physics* **94**, 3883–3890 (2003).
  17. D. Knoll, B. Heinemann, and K.-E. Ewald, “Comparison of SiGe and SiGe:C Heterojunction Bipolar Transistors,” *Thin Solid Films* **369**, 342–346 (2000).